Exosomal STAT1 derived from high phosphorus-stimulated vascular endothelial cells induces vascular smooth muscle cell calcification via the Wnt/β-catenin signaling pathway

ZHENG QIN[1,2], YUPEI LI[1,2], JIAMENG LI[1,2], LUOJIA JIANG[1,2], ZHUYUN ZHANG[1,2], KAIXI CHANG[1,2], QINBO YANG[1,2], SHANSHAN CHEN[1,2], RUOXI LIAO[1,2] and BAIHAI SU[1,2]

[1]Department of Nephrology, National Clinical Research Center for Geriatrics, West China Hospital;
[2]Med+ Biomaterial Institute, West China Hospital/West China School of Medicine,
Sichuan University, Chengdu, Sichuan 610041, P.R. China

Abstract. Vascular calcification is commonly observed in chronic kidney disease. The mechanism of how the calcification signal from endothelial cells is transmitted to vascular smooth muscle cells (VSMCs) remains unknown. The aim of the present study was to investigate whether exosomes from HUVECs (HUVEC-Exos) could regulate VSMC calcification and its potential signaling pathway. HUVEC-Exos were isolated from HUVECs under no phosphorus (NP) and high phosphorus (HP) conditions. Alizarin Red S staining and calcium (Ca) content analysis were carried out to detect calcification in VSMCs. Proteomics analysis was carried out to detect the differential expression of exosomal proteins. Protein and mRNA levels were measured by western blot analysis and reverse transcription-quantitative PCR (RT-qPCR). Exosomes derived from HP-HUVECs promoted the calcification of VSMCs, as assessed by Alizarin Red S staining, alkaline phosphatase activity assays, Ca content measurements and the increased expression of runt-related transcription factor 2 and osteopontin. Proteomic analysis detected the upregulation of STAT1 in HP-exosomes from HUVECs (HUVEC-Exos) compared with NP-HUVEC-Exos, which was also confirmed by western blot analysis and RT-qPCR. Inhibition of STAT1 expression in VSMCs using fludarabine or knockdown of STAT1 expression using small interfering RNA alleviated the calcification of VSMCs. Furthermore, lithium chloride (Wnt activator) reversed the protective effect of STAT1 inhibition on VSMC calcification, while Dickkopf-1 (Wnt inhibitor) exerted the opposite effect, suggesting that activation of the Wnt/β-catenin signaling pathway was involved in STAT1-mediated VSMC calcification. In conclusion, the present results indicated that exosomal STAT1 derived from HP-treated HUVECs could promote VSMC calcification, and activation of the Wnt/β-catenin pathway may be a potential mechanism of the VSMC calcification promoted by exosomes.

Introduction

Vascular calcification (VC) is characterized by the abnormal deposition of minerals in the wall of blood vessels and is commonly observed in patients with chronic kidney disease (CKD) (1). VC can be divided into intima calcification and media calcification according to the calcified site, of which the VC characteristic in patients with CKD mostly involves the tunica media (2). Calcification of the tunica media leads to an increase in vascular stiffness and decreased compliance, resulting in higher pulse pressure, left ventricular hypertrophy, and changes in left ventricular pressure and coronary perfusion (3). It has been demonstrated that VC is associated with an increase in all-cause mortality, especially from cardiovascular causes, such as ischemic heart disease (4-6). Although several medications may ease the progression of VC, there is still no proven treatment for it in clinical practice (7). Therefore, early prevention and treatment of VC have important clinical significance for reducing cardiovascular complications and improving the prognosis of patients with CKD.

VC is considered to be an active, tunable physiological process that involves abnormalities in calcium (Ca) and phosphorus metabolism and differentiation of vascular smooth muscle cells (VSMCs) (1,2,8). Intima calcification usually starts from atherosclerotic plaques, while early medial calcification begins at focal medial calcification and gradually expands to whole-vessel calcification (2). VC has been previously considered to occur at the end stage of CKD (9); however, epidemiological studies have suggested that VC could also be observed even at the early stage of CKD, which is mainly characterized by abnormal blood biochemistry (10-12). How

Correspondence to: Dr Ruoxi Liao or Dr Baihai Su, Department of Nephrology, National Clinical Research Center for Geriatrics, West China Hospital, Sichuan University, 37 Guoxue Lane, Wuhou, Chengdu, Sichuan 610041, P.R. China
E-mail: liaoruoxi@wchscu.cn
E-mail: subaihai@scu.edu.cn

these abnormal signals are transmitted to VSMCs in the tunica media through the intima of vessels and then initiate the whole process of VC remains to be elucidated.

Exosomes, a type of extracellular vesicle (EV) with a diameter of 30-200 nm, can carry bioactive molecules, including proteins, nucleic acids and lipids, and serve a role in signal transmission between adjacent cells or distal cells, which can be widely found in body fluids, including blood and urine (13). Exosomes have been reported to participate in VC through various mechanisms (14). Pan *et al* (15) added exosomes extracted from a VC mouse model to VSMCs and found that they also began to express calcification-related proteins, suggesting that the calcification signal could be transmitted between VSMCs through exosomes. Li *et al* (16) found that exosomes secreted by high glucose-stimulated vascular endothelial cells (ECs) promoted aging and Ca deposition in VSMCs, suggesting that exosomes may serve a role in diabetes-related VC. The interplay between ECs and VSMCs is the main driver of vascular pathological changes, which also serve a key role in the process of VC (14,17). Most studies have focused on the effects of pathological stimuli on ECs, which compose the inner layer of blood vessels, since they are directly stimulated by factors such as hyperglycemia (16,18-20). Liu *et al* (19) reported that the effect of ECs on VSMC calcification was achieved by secreting soluble factors such as cholestane-3β, 5α and 6β-triol, demonstrating the roles of ECs in VC modulated by oxysterols in atherosclerotic plaques. Hyperglycemia-stimulated ECs release exosomal Notch3 and versican, which can be taken up by VSMCs and linked to their calcification/senescence, indicating the role of exosomes in extracellular communication (16,20). Therefore, we hypothesized that abnormal biochemical factors in the early stage of CKD, especially higher phosphorus, could stimulate vascular ECs and transmit this abnormal signal to the tunica media through exosomes, initiating the process of VC in CKD.

The present study explored the role and mechanism of exosomes derived from high phosphorus (HP)-stimulated HUVECs in regulating VSMC calcification. The aims of the present study were to investigate whether HP-HUVEC-Exos could promote VSMC calcification and to determine which contents of HP-HUVEC-Exos may serve a role in regulating calcification and its potential signaling pathway.

Materials and methods

Cell culture and transfection. Human aortic VSMCs were purchased from American Type Culture Collection (ATCC-CRL-1999) and HUVECs were purchased from iCell Bioscience, Inc. VSMCs were cultured in DMEM (Gibco; Thermo Fisher Scientific, Inc.) supplemented with 10% FBS (MilliporeSigma) and 1% penicillin/streptomycin. HUVECs were cultured in ECM medium (ScienCell Research Laboratories, Inc.) with 10% FBS (MilliporeSigma) and 1% penicillin/streptomycin. Cells were cultured at 37°C in a humidified atmosphere with 5% CO_2 and passaged every 2-3 days.

For cell transfection, STAT1 small interfering RNA (si-STAT1; cat. no. stB0000954A) and si-negative control (si-NC; cat. no. siN0000001-1-5; the sequence is not publicly available) oligos (Guangzhou RiboBio Co., Ltd.), and STAT1 overexpression (o/e) and its negative control (NC) plasmids

based on the backbone of pCMV3-C-HA (Sino Biological, Inc.) were transfected into VSMCs using Lipofectamine 2000 (Invitrogen; Thermo Fisher Scientific, Inc.) at a final concentration of 50 nM. Briefly, VSMCs were plated at a density of $5x10^5$ cells in 6-well plates and cultured at 37°C with 5% CO_2. When they reached 50% confluence, cells were transfected with specific siRNA or plasmids with Lipofectamine 2000 (Invitrogen; Thermo Fisher Scientific, Inc.) according to the manufacturer's instructions. After 6 h of transfection with opti-MEM at 37°C with 5% CO_2, the DMEM containing 10% FBS was replaced. After 24 h following transfection, the cells were used for subsequent experimentation. The target sequences of si-STAT1 are listed in Table SI.

For some experiments verifying whether Wnt/β-catenin pathway was involved in VSMC calcification, VSMCs were transfected with the overexpression plasmids of STAT1 (STAT1 o/e group) and its controls (STAT1-NC group), si-STAT1 (si-STAT1 group) and its controls (si-NC group) under NP conditions at 37°C with 5% CO_2. After the knockdown or overexpression of STAT1 by siRNA or plasmid, VSMCs were cultured in DMEM with 3 mM phosphorus for 7 days at 37°C with 5% CO_2 to induce calcification. For the last 3 days of this period, lithium chloride (LiCl; 5 mmol/l; Sigma-Aldrich; Merck KGaA) was added to the medium of the si-STAT1 group (si-STAT1 + LiCl group) to activate the Wnt/β-catenin pathway and Dickkopf-1 (Dkk-1; 100 ng/ml; MedChemExpress) was added to the medium of the STAT1 o/e group (STAT1 o/e + Dkk-1 group) to inhibit the Wnt/β-catenin pathway at 37°C with 5% CO_2.

Isolation of exosomes from HUVECs. HUVECs were cultured in DMEM with the addition of NaH_2PO_4 for the HP (3 mM; pH=7.4) group or without NaH_2PO_4 for the no phosphorus (NP) group for 48 h at 37°C in a humidified atmosphere with 5% CO_2 for exosome isolation. NaH_2PO_4 (MilliporeSigma) was used to increase the concentration of phosphorus in the medium. Before extraction of exosomes from HUVECs, the cells were cultured with medium supplemented with 10% exosome-depleted FBS for 48 h at 37°C with 5% CO_2 (C38010100; Shanghai VivaCell Biosciences, Ltd.).

Exosomes were concentrated using an ExoQuick-TC Exosome Precipitation Solution kit (EXOTC10A; System Biosciences, LLC). This method has been widely used before and has been proven to collect exosomes effectively (21-23). Briefly, the supernatant was centrifuged at room temperature as follows: 300 x g for 10 min, 2,000 x g for 30 min and 10,000 x g for 30 min. An Amicon Ultra15 Centrifugal Filter Unit (100 kDa; MilliporeSigma) was used to concentrate the supernatant. The ultrafiltration liquid and exosome isolation reagents were mixed at a 5:1 ratio and incubated at 4°C for ~16 h. Finally, the mixture was centrifuged at room temperature at 1,500 x g for 30 min, and the exosome pellets were resuspended in 200 μl PBS. Protein quantification of exosomes was performed using a BCA kit (Beyotime Institute of Biotechnology).

Identification of exosomes. Transmission electron microscopy (TEM) was used to observe the morphology of exosomes. Briefly, exosomes were fixed with equal volumes of 1% phosphotungstic acid (pH=7.4) at room temperature for 30 min.

After rinsing, 10 μl of the sample was loaded onto a bronze net with film and left for 10 min at room temperature. Then, 10 μl uranyl dioxyacetate was added to the bronze net to precipitate for 10 min at room temperature, and the floating liquid was absorbed by filter paper at room temperature. Finally, images were observed under a Hitachi HT7760 transmission electron microscope (Hitachi, Ltd.) at 100 kV. The size distribution of the exosomes was measured by dynamic light scattering using nanoparticle tracking analysis (NTA; Zetasizer Nano ZS; Malvern Instruments, Inc.). The expression levels of the exosomal surface marker proteins CD63 (ab68418; Abcam) and CD9 (ab223052; Abcam) were analyzed by western blot analysis, which was performed as described subsequently.

Exosome uptake by VSMCs. Exosomes were labeled with a PKH26 Red Fluorescent Cell Linker kit (UR52302; Umibio Science and Technology Group) according to the manufacturer's instructions. Briefly, labeling dye was added to the exosomes resuspended in PBS and incubated at room temperature with shaking for 10 min. Then, the tube was spun at 100,000 x g for 17 min at room temperature, and the exosome pellet was resuspended in PBS. Labeled exosomes were incubated with VSMCs for 0 and 24 h at 37°C with 5% CO_2, and then the cells were fixed with 4% paraformaldehyde at room temperature for 10 min and washed three times with PBS. DAPI (Invitrogen; Thermo Fisher Scientific, Inc.) was added at room temperature for 5 min. After washing the cells with PBS three times, the staining signals were analyzed with ZEN 2012 microscopy software (blue edition; Carl Zeiss AG) using confocal microscopy (DMI600B; Leica Microsystems GmbH).

Measurement of VSMC calcification. To induce calcification, VSMCs were co-cultured with HUVEC-Exos for 14 days (10,000 cells were treated with 5 μg HUVEC-Exos continuously). For the control group, VSMCs were cultured with normal DMEM without the addition of HUVEC-Exos. Alizarin Red S staining, alkaline phosphatase (ALP) activity assays and Ca content measurements were conducted to determine the calcification condition.

Alizarin Red S staining was conducted to assess VSMC calcification. Cells were washed twice with PBS, fixed in 4% paraformaldehyde for 30 min at room temperature and then stained with 0.2% Alizarin Red (pH=8.3; Beijing Solarbio Science & Technology Co., Ltd.) for 20 min at room temperature. Subsequently, the cells were washed with PBS, and mineralized nodules were assessed and images were captured using a light microscope (Carl Zeiss AG) and analyzed with ZEN 2012 microscopy software (blue edition; Carl Zeiss AG).

ALP activity was detected using an ALP kit purchased from Beyotime Institute of Biotechnology (P0321S) according to the manufacturer's instructions. Spectrophotometric measurement of p-nitrophenol release was utilized. ALP activity was normalized to the total protein content of the cell lysate.

The Ca content was quantified using a Ca content kit obtained from Nanjing Jiancheng Bioengineering Institute (C004-2-1) according to the manufacturer's instructions.

The expression levels and mRNA levels of runt-related transcription factor 2 (Runx2) and osteopontin (OPN) were detected using western blotting at the protein level and reverse transcription-quantitative PCR (RT-qPCR) at the gene level. All experiments were performed as described subsequently.

RT-qPCR. Total RNA was extracted from cells using a total RNA isolation kit (Vazyme Biotech Co., Ltd.) according to the manufacturer's instructions. Complementary DNA was synthesized using HiScript II Q Select RT SuperMix for qPCR (Vazyme Biotech Co., Ltd.) according to the manufacturer's instructions. For RT-qPCR analysis, GAPDH was used as the reference. The mRNA levels of Runx2, OPN, Wnt-3a and β-catenin were analyzed using RT-qPCR and SYBR Green Supermix (Vazyme Biotech Co., Ltd.). The thermocycling conditions were: i) Incubation step of 30 sec at 90°C; ii) 40 cycles of 10 sec at 95°C and 30 sec at 60°C; and iii) 15 sec at 95°C, 60 sec at 60°C and 15 sec at 95°C. The primers were synthesized by TsingKe Biological Technology, and the sequences are listed in Table I. All treatments and conditions were performed in triplicate to calculate the statistical significance, and the results were calculated using the $2^{-\Delta\Delta Cq}$ method (24).

Western blot analysis. Total protein was extracted from cells using radioimmune precipitation assay lysis buffer (Beyotime Institute of Biotechnology) supplemented with protease inhibitor cocktail and phosphatase inhibitor cocktail (Bimake). The protein concentrations were determined using a BCA protein assay kit (Biosharp Life Sciences) and 30 μg protein was loaded per lane. Equal amounts of protein lysate were separated by 10-12% SDS-PAGE in Tris/SDS buffer and then transferred onto polyvinylidene difluoride membranes (MilliporeSigma). The membranes were blocked in 5% nonfat milk (w/v) in Tris-buffered saline with 0.1% Tween-20 for 1 h at room temperature and incubated with the corresponding primary antibodies at 4°C overnight. After washing, the membranes were further incubated with HRP-conjugated secondary antibodies (1:10,000) at room temperature for 1 h. The immunoreactive bands were evaluated to visualize the expression of designated proteins using the chemiluminescence detection system through the peroxidase reaction, and the images of the bands were recorded with the Chemi Doc MP imaging system (Bio-Rad Laboratories, Inc.). The chemiluminescence substrate reagent (cat. no. 4AW011-100) was purchase from Beijing 4A Biotech Co., Ltd. GAPDH was used as the internal loading control. The films were analyzed with Image Lab software 6.0.1 (Bio-Rad Laboratories, Inc.). All experiments were repeated at least three times. The primary antibodies used in the present study were as follows: Anti-GAPDH (ab8245; Abcam; 1:2,000), anti-CD63 (ab217345; Abcam; 1:1,000), anti-CD9 (ab223052; Abcam; 1:1,000), anti-OPN (ab8245; Abcam; 1:1,000), anti-Runx2 (A11753; ABclonal Biotech Co., Ltd.; 1:1,000), anti-STAT1 (T55227; Abmart Pharmaceutical Technology Co., Ltd.; 1:2,000), anti-Wnt-3a (M63350; Abmart Pharmaceutical Technology Co., Ltd.; 1:1,000) and anti-β-catenin (A19657; ABclonal Biotech Co., Ltd.; 1:1,000). The secondary antibodies were as follows: Goat Anti-Mouse IgG H&L (HRP; ab205719; Abcam; 1:10,000) and Goat Anti-Rabbit IgG H&L (HRP; ab205718; Abcam; 1:10,000).

Proteomics analysis. The HUVEC-Exos samples were processed for label-free-based quantitative proteomic analysis by Shanghai Huaying Biomedical Technology Co., Ltd. The

Table I. Sequences of the primers for reverse transcription-quantitative PCR.

Human gene	Sequence (5'-3')
F-OPN	AATCTCCTAGCCCCACAGACC
R-OPN	CCACACTATCACCTCGGCCA
F-Runx2	GCGGTGCAAACTTTCTCCAG
R-Runx2	TGTCACTGTGCTGAAGAGGC
F-GAPDH	AATGGGCAGCCGTTAGGAAA
R-GAPDH	GCGCCCAATACGACCAAATC
F-STAT1	CAAGTGTTATGGGACCGCAC
R-STAT1	CTCTCATTCACATCTCTCAACTTCA
F-Wnt-3a	GTGTTCCACTGGTGCTGCTA
R-Wnt-3a	CCCTGCCTTCAGGTAGGAGT
F-β-catenin	CTGAGGAGCAGCTTCAGTCC
R-β-catenin	GGCCATGTCCAACTCCATCA

F, forward; OPN, osteopontin; R, reverse; Runx2, runt-related transcription factor 2.

proteomic content of HUVEC-Exos in HP and NP conditions was compared using high-performance liquid chromatography tandem mass spectrometry at room temperature. Briefly, 2 μg samples (2-3 μl in volume) for each group were taken and separated by Easy-NLC1000 (Thermo Fisher Scientific, Inc.) using an analytical column (C18; 1.9 μm; 75 μm x 20 cm; Thermo Fisher Scientific, Inc.) at a mobile solution flow rate of 200 nl/min. The mobile phase A was 0.1% formic acid (FA) in water (v/v) and mobile phase B was 0.1% FA in acetonitrile (v/v). The analysis time for each sample was 120 min and gradient elution was used (v/v; 0-5 min, 2-8% mobile phase B; 5-90 min, 8-24% mobile phase B; 90-110 min, 24-32% mobile phase B; 110-115 min, 32-90% mobile phase B; 115-120 min, 90% mobile phase B). Since label-free quantitative methods were used, no internal standards were used in the present study. The mass spectrometer was an Orbitrap Fusion Lumos (Thermo Fisher Scientific, Inc.). Tandem mass spectrometry was performed using Data Dependent Acquisition mode. The full sweep resolution was 60,000 full width at half maxima, the mass/charge ratio range was set to M/Z 350-1,600, and the collision energy was set to 30% in higher energy collisioninduced dissociation mode. All raw files were converted into mgf files and searched against the Swissprot database using Proteome Discoverer2.4 (Sequent HT; Thermo Fisher Scientific, Inc.). Taxonomy was selected as Homo sapiens. Enzyme was selected as trypsin. Fixed modifications were set as Carbamidomethyl (C). Variable modifications were set as Oxidation (M), Acetyl (Protein N-term), Met-loss+Acetyl (M), Met-loss (M). Max Missed Cleavages was 2. Target FDR (Strict) was set as 0.01, and target FDR (Relaxed) was set as 0.05. Min. peptide Length was set as 6. Mass Tolerance was 10 ppm. For normalizing the different protein abundances in different experiments, the protein precursor intensity was calculated and then median-normalized. All further analyses were based on the normalized results. Differentially expressed proteins were identified with a cutoff of absolute fold change ≥4. For each category, a two-tailed Fisher's exact test was employed

to test the enrichment of the differentially expressed proteins against all identified proteins. A two-tailed P-value <0.05 was considered significant. The mass spectrometry proteomics data have been deposited to the ProteomeXchange Consortium (http://proteomecentral.proteomexchange.org) via the iProX (http://www.iprox.org) partner repository with the dataset identifier PXD036925.

Statistical analysis. The results of the experiments are presented as the mean ± SD, and the analysis was performed using SPSS software (version 21.0; IBM Corp.). One-way ANOVA followed by Tukey's post hoc test was employed to evaluate the significance of differences among multiple groups. All experiments were repeated at least three times, and representative experimental data are shown in the figures. P<0.05 was considered to indicate a statistically significant difference.

Results

Identification of exosomes. Exosomes were isolated from the supernatant of HUVECs. NTA and TEM were used to characterize the vesicles. TEM indicated that these vesicles had a typical bilayer structural morphology (Fig. 1A). Western blot analysis further indicated the presence of exosome markers (including CD9 and CD63) in the HUVEC-Exo group, while almost no expression of CD9 and CD63 was observed in the HUVEC group (Fig. 1B). NTA demonstrated that these vesicles had a diameter of 80-170 nm (Fig. 1C). The typical bilayer structural morphology, expression of exosome markers (CD9 and CD63) and the diameter of 80-170 nm confirmed that these vesicles were exosomes.

HP-HUVEC-Exos induce VSMC calcification. To explore the ability of HUVEC-Exos to regulate VSMC calcification, VSMCs were co-cultured with HP-HUVEC-Exos and NP-HUVEC-Exos. For the control (Ctrl) group, VSMCs were cultured with normal DMEM in the absence of HUVEC-exosomes.

First, the present study examined whether HUVEC-Exos could be taken up by VSMCs. Exosomes were labelled with PKH26, and HUVECs were incubated with the labeled exosomes for 0 and 24 h. Fluorescence microscopy revealed that PKH26-labeled HUVEC-Exos could be taken up by VSMCs (Fig. 1D). VSMCs were further incubated with HP-HUVEC-Exos, NP-HUVEC-Exos or without exosomes. Compared with VSMCs treated with NP-HUVEC-Exos and without exosomes, HP-HUVEC-Exos could induce VSMC calcification. The protein expression levels of both Runx2 and OPN were significantly upregulated in the HP-HUVEC-Exos group compared with the other two groups (Fig. 2A), as were the Runx2 and OPN mRNA levels (Fig. 2B). The results of ALP activity and Ca content measurements also revealed that HP-HUVEC-Exos could induce the calcification of VSMCs (Fig. 2C and D). In addition, Alizarin Red S staining showed that mineralized nodules were greatly increased in VSMCs treated with HP-HUVEC-Exo for 14 days (Fig. 2E). The present results suggested that exosomes derived from HP-stimulated HUVECs could promote the calcification of VSMCs.
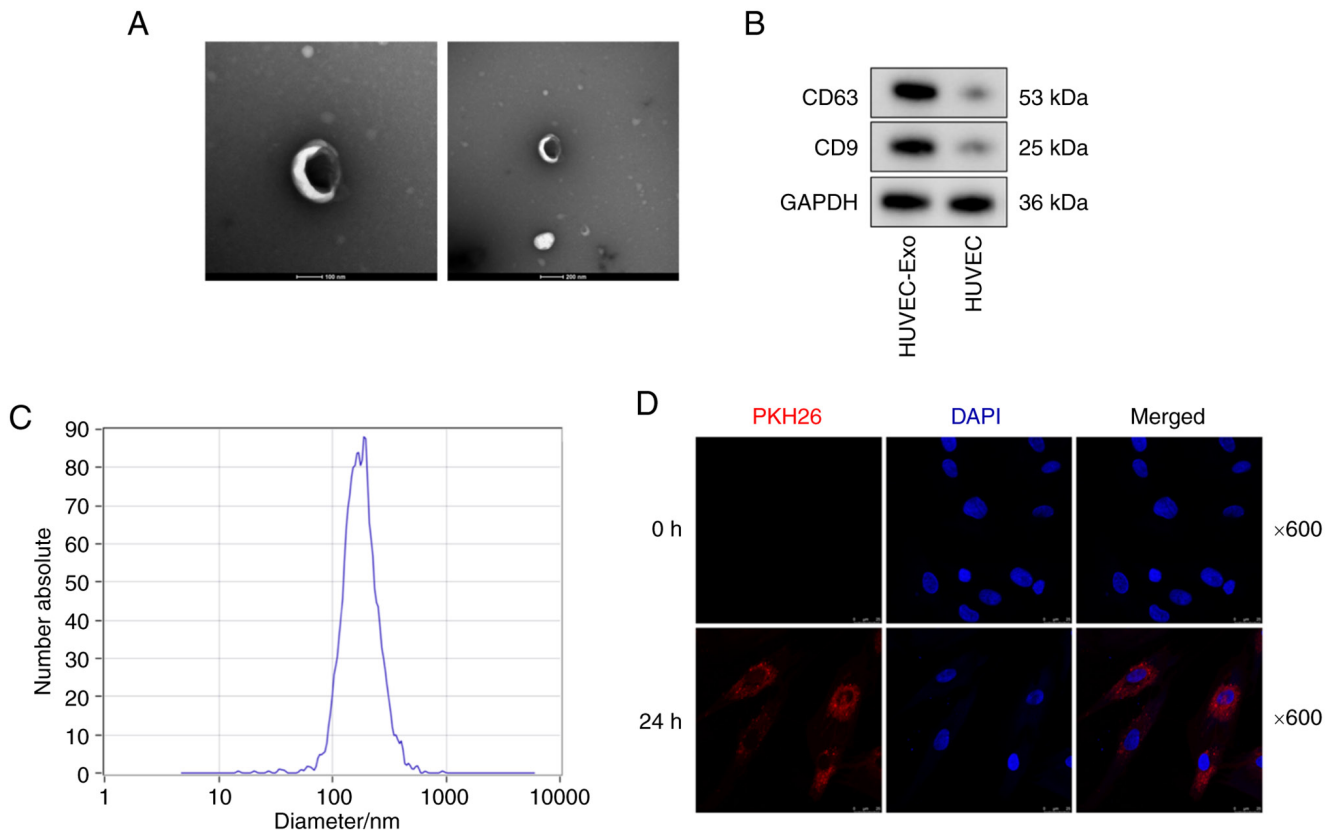
Figure 1. Exosomes were identified and taken up by VSMCs. (A) Transmission electron microscopy was used to assess the morphology of exosomes. Scale bar, 100 nm (left) or 200 nm (right). (B) Exosome-specific markers were detected by western blot analysis. (C) Nanoparticle tracking analysis of exosomes derived from VSMCs showed that the size of most HUVEC-Exos was 80-170 nm. (D) VSMCs were incubated with PKH26 fluorescently labeled exosomes for 0 and 24 h. Confocal microscopy analyses was used to identify the uptake of exosomes by VSMCs (PKH26 in red; DAPI in blue). Magnification, x600. HUVEC-Exos, exosomes from HUVECs; VSMC, vascular smooth muscle cell.
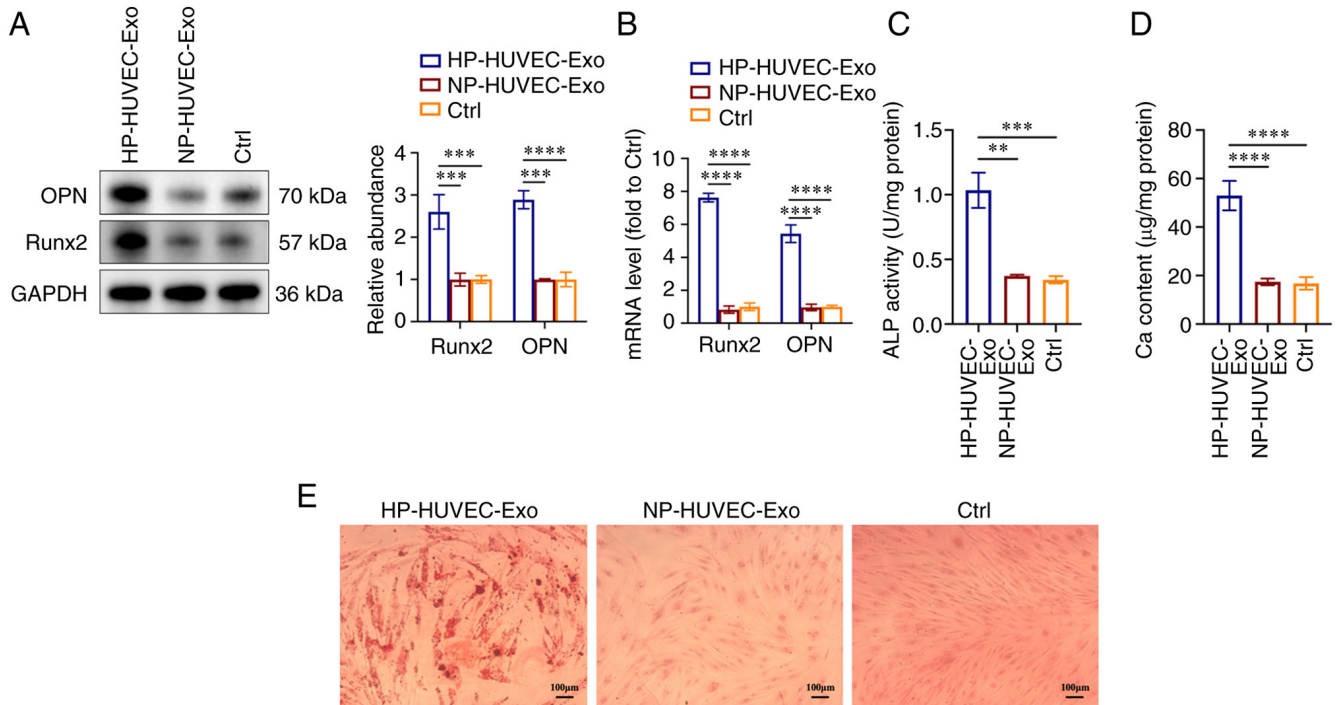
Figure 2. HP-stimulated HUVEC-Exos promote VSMC calcification. (A) Expression levels of OPN and Runx2 in VSMCs were measured by western blot analysis. (B) Reverse transcription-quantitative PCR analysis of OPN and Runx2 expression in VSMCs. (C) ALP activity assays were performed. (D) Ca content in VSMCs was measured. (E) VSMCs were stained for mineralization using Alizarin red S. Scale bar, 100 μm. $**P<0.01$, $***P<0.001$, $****P<0.0001$ compared with the Ctrl group. ALP, alkaline phosphatase; Ca, calcium; Ctrl, control; HP, high phosphorus; HUVEC-Exos, exosomes from HUVECs; NP, no phosphorus; OPN, osteopontin; Runx2, runt-related transcription factor 2; VSMC, vascular smooth muscle cell.
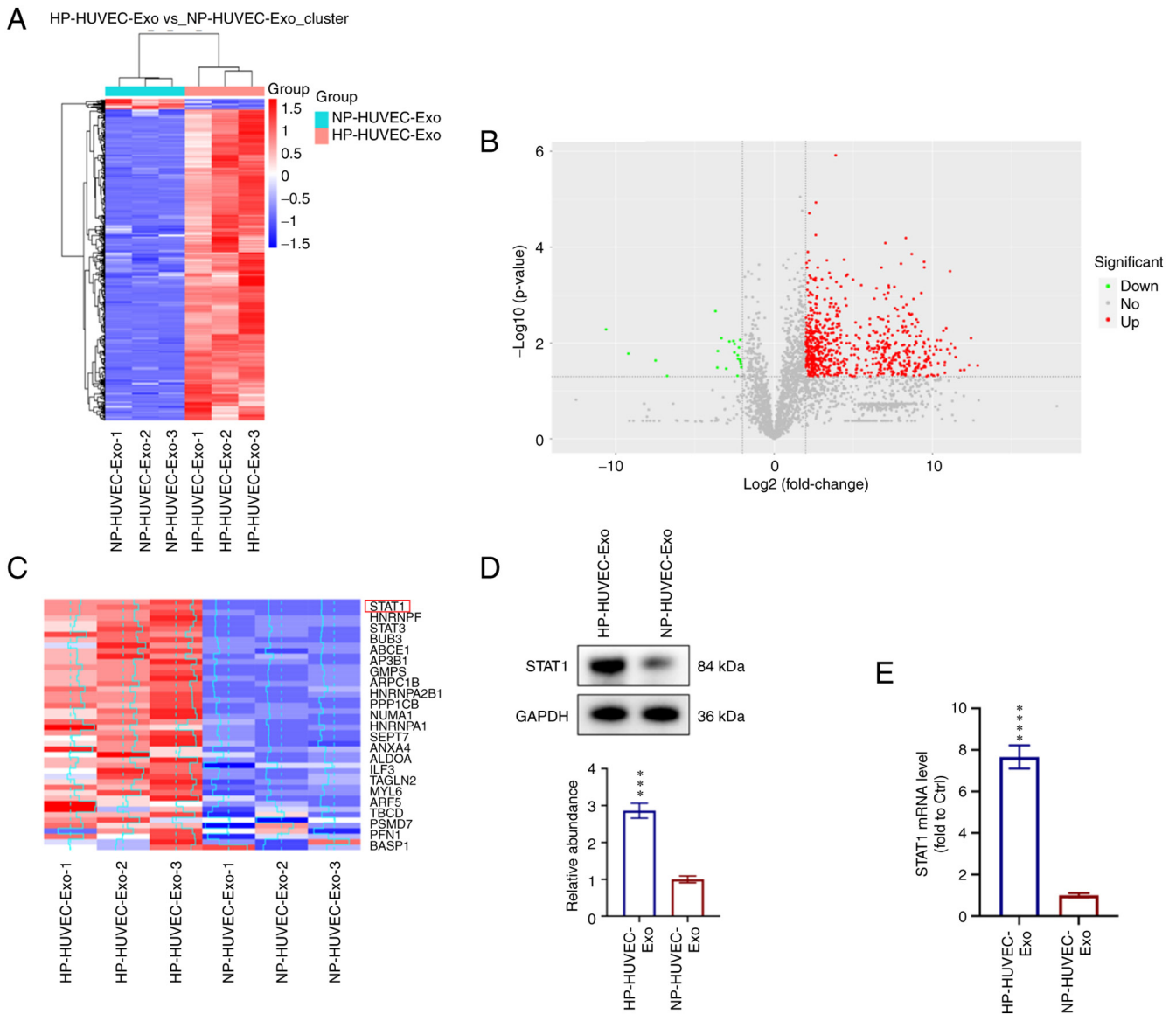
Figure 3. STAT1 is enriched in HP-HUVEC-Exos. (A) Heat map of 719 differentially expressed proteins (cutoff, fold change ≥4 and P<0.05) between HP-HUVEC-Exos and NP-HUVEC-Exos according to proteomics analysis. (B) Volcano plots of 719 differentially expressed proteins. (C) Different expression levels of STAT1 in HP-HUVEC-Exos and NP-HUVEC-Exos according to proteomics analysis. (D) Expression levels of STAT1 in VSMCs treated with HP-HUVEC-Exos and NP-HUVEC-Exos were determined by western blot analysis. (E) Reverse transcription-quantitative PCR analysis of STAT1 expression in VSMCs. ***P<0.001, ****P<0.0001 compared with the NP-HUVEC-Exos group. Ctrl, control; HP, high phosphorus; HUVEC-Exos, exosomes from HUVECs; NP, no phosphorus; VSMC, vascular smooth muscle cell.

STAT1 is enriched in HP-HUVEC-Exos and involved in regulating VSMC calcification. To explore the molecular mechanisms of HP-HUVEC-Exos in VSMC calcification, proteomic analysis using label-free technology was conducted to detect the differentially expressed proteins between HP-HUVEC-Exos and NP-HUVEC-Exos. A total of 719 differentially expressed proteins were identified, among which 697 proteins were significantly upregulated and 22 proteins were downregulated in HP-HUVEC-Exos compared with NP-HUVEC-Exos (Fig. 3A and B). Based on the results of proteomic analysis, STAT1 expression was significantly different between HP-HUVEC-Exos and NP-HUVEC-Exos. The present study focused on the different expression and potential role of STAT1 protein in VSMC calcification (Fig. 3C). HP treatment was associated with a significant upregulation of STAT1 in HUVEC-Exos. Furthermore, western blot analysis

confirmed the enrichment of STAT1 in HP-HUVEC-Exos (Fig. 3D). In addition, STAT1 mRNA expression was significantly upregulated in VSMCs treated with HP-HUVEC-Exos compared with those treated with NP-HUVEC-Exos (Fig. 3E).

To further investigate the role of STAT1 in VSMC calcification, fludarabine (an inhibitor of STAT1) was used to inhibit STAT1 expression in VSMCs. Compared with the HP-HUVEC-Exos group, both western blotting and RT-qPCR analyses showed that the expression levels of Runx2 and OPN were significantly downregulated in the HP-HUVEC-Exos + fludarabine group (Fig. 4A and B). Alizarin Red S staining demonstrated that mineralized nodules were greatly decreased in VSMCs treated with HP-HUVEC-Exos + fludarabine compared with VSMCs treated with HP-HUVEC-Exos (Fig. 4C). The results of ALP activity and Ca content measurements also demonstrated that the inhibition of
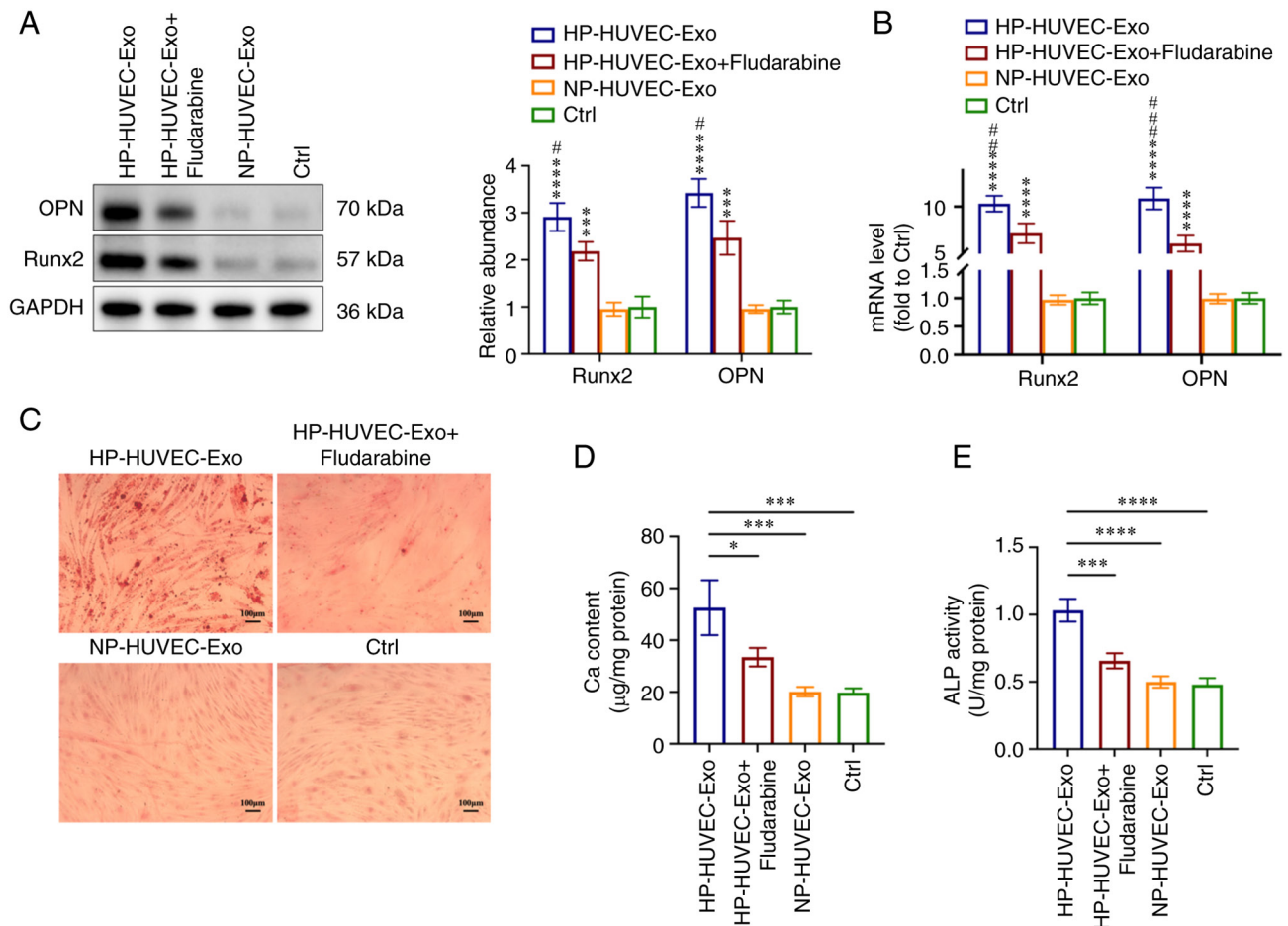
Figure 4. STAT1 is involved in HP-HUVEC-Exos-induced VSMC calcification. VSMCs were treated with HP-HUVEC-Exos, HP-HUVEC-Exos + fluda-rabine, NP-HUVEC-Exos or fresh conditioned medium (Ctrl group) for 14 days. (A) Expression levels of OPN and Runx2 in VSMCs were measured by western blot analysis. (B) Reverse transcription-quantitative PCR analysis of OPN and Runx2 expression in VSMCs. (C) Alizarin Red S staining revealed mineralization. Scale bar, 100 μm. (D) Ca content in VSMCs was measured. (E) ALP activity was tested. *P<0.05, ***P<0.001, ****P<0.0001 compared with the Ctrl group. $^#$P<0.05, $^{##}$P<0.01, $^{###}$P<0.001 compared with the HP-HUVEC-Exos + fludarabine group. ALP, alkaline phosphatase; Ca, calcium; Ctrl, control; HP, high phosphorus; HUVEC-Exos, exosomes from HUVECs; NP, no phosphorus; OPN, osteopontin; Runx2, runt-related transcription factor 2; VSMC, vascular smooth muscle cell.

STAT1 by fludarabine alleviated HP-HUVEC-Exo-induced VSMC calcification (Fig. 4D and E). Overall, the ability of HP-HUVEC-Exos to induce VSMC calcification was decreased when STAT1 was suppressed.

Inhibition of STAT1 alleviates HP-induced VSMC calcification via the Wnt/β-catenin pathway. The present study further explored the role of STAT1 in VSMC calcification. First, VSMCs were transfected with si-STAT1 to suppress STAT1 expression and with si-NC. The knockdown effect of si-STAT1 on the protein levels of STAT1 was measured by western blotting (Fig. 5A). Based on the downregulation effect, si-STAT1-01 was selected for further experiments. VSMCs were incubated with HP (3 mM) to induce calcifica-tion or fresh conditional medium (Ctrl) simultaneously. When the expression of STAT1 was knocked down, the effect of HP on VSMC calcification was almost abolished, as evidenced by the decreased expression levels of OPN and Runx2 in the HP + si-STAT1 group compared with the HP group, which were analyzed by western blotting and RT-qPCR (Fig. 5B and C). Furthermore, the mineralized nodules were also reduced when STAT1 was downregulated in the HP + si-STAT1 group

compared with the HP group (Fig. 5D). The Ca content and ALP activity measurements also revealed that the inhibi-tion of STAT1 alleviated HP-induced VSMC calcification (Fig. 5E and F).

In addition, the expression levels of Wnt/β-catenin pathway-related proteins were detected. Wnt-3a and β-catenin were significantly upregulated in calcification VSMCs (HP, HP + si-STAT1 and HP + si-NC groups) compared with the Ctrl group, and the inhibition of STAT1 (HP + si-STAT1 group) also suppressed the expression of Wnt-3a and β-catenin both at the protein and mRNA levels compared with the HP group (Fig. 5G and H). These results indicated that STAT1 was involved in HP-induced VSMC calcification, and the activation of the Wnt/β-catenin pathway may be the potential mechanism.

Wnt/β-catenin signaling pathway is involved in STAT1-mediated VSMC calcification. To verify whether STAT1 affected VSMC calcification via the Wnt/β-catenin pathway, VSMCs were transfected with the overexpres-sion plasmids of STAT1 (STAT1 o/e group) and its controls (STAT1-NC group) under NP conditions. Western blot analysis
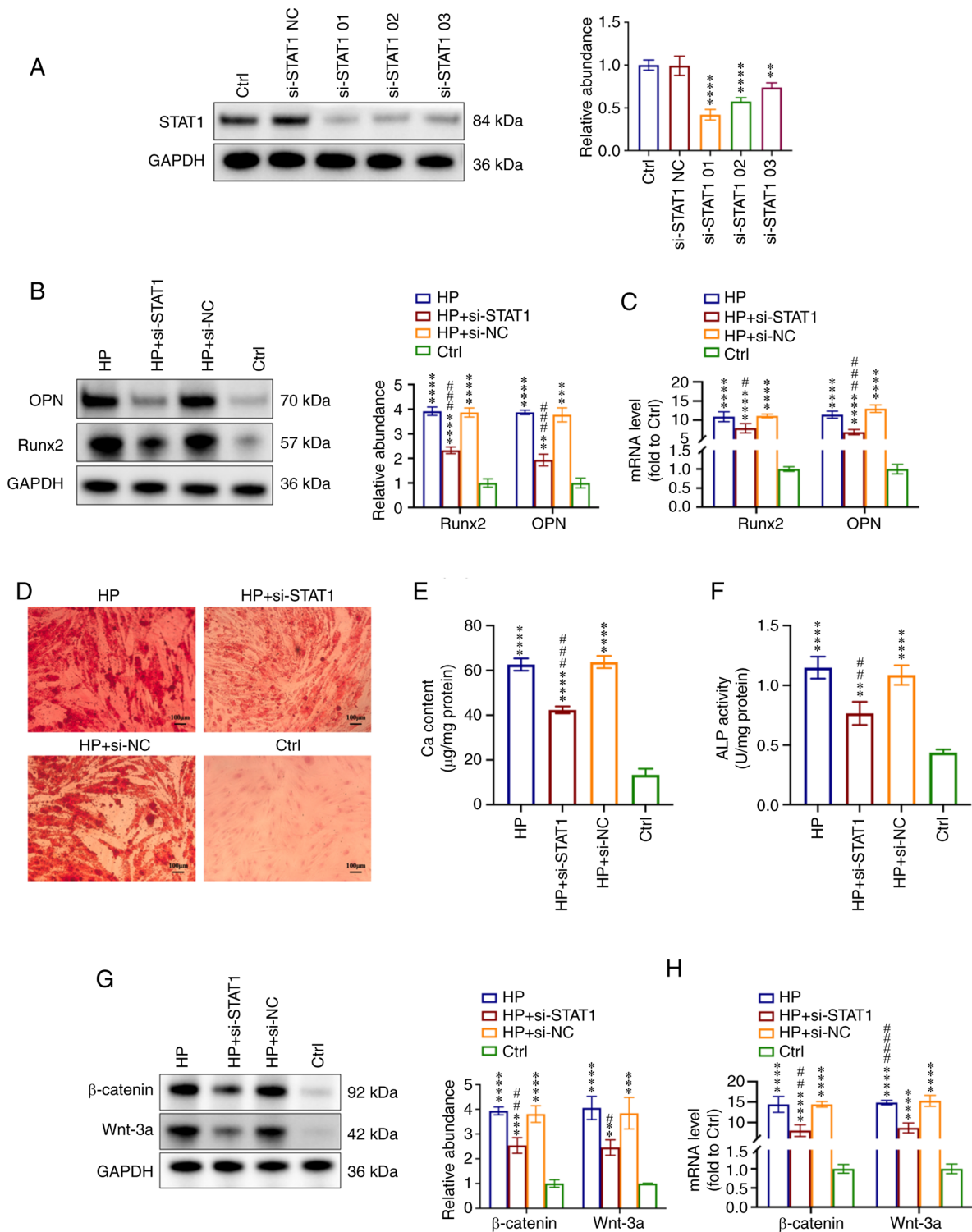
Figure 5. STAT1 inhibition alleviates HP-induced VSMC calcification via the Wnt/β-catenin signaling pathway. VSMCs were treated with si-STAT1 and si-NC and then incubated with HP (3 mM) to induce calcification or fresh conditioned medium (Ctrl) for 7 days. (A) Effect of si-STAT1 on protein levels of STAT1. Based on the knockdown effect, si-STAT1-01 was selected for further experiments. (B) Expression levels of OPN and Runx2 were measured by western blot analysis in VSMCs. (C) RT-qPCR analysis of OPN and Runx2 mRNA expression in VSMCs. (D) Alizarin Red S staining indicated the mineralization. Scale bar, 100 μm. (E) Ca content in VSMCs was measured. (F) ALP activity was tested. (G) Expression levels of Wnt-3a and β-catenin were measured by western blot analysis. (H) RT-qPCR analysis of Wnt-3a and β-catenin expression in VSMCs. **P<0.01, ***P<0.001, ****P<0.0001 compared with the Ctrl group. $^{#}$P<0.05, $^{##}$P<0.01, $^{###}$P<0.001, $^{####}$P<0.0001 compared with the HP group. ALP, alkaline phosphatase; Ca, calcium; Ctrl, control; HP, high phosphorus; NC, negative control; OPN, osteopontin; RT-qPCR, reverse transcription-quantitative PCR; Runx2, runt-related transcription factor 2; si, small interfering RNA; VSMC, vascular smooth muscle cell.

demonstrated the overexpression of STAT1 in VSMCs after transfection (Fig. 6A). Subsequently, an activator or inhibitor of the Wnt/β-catenin signaling pathway was used for the treatment

of HP-treated VSMCs. Briefly, STAT1-overexpressing VSMCs were treated with 3 mM phosphorus for 7 days, with or without 100 ng/ml Dkk-1 (Wnt inhibitor) added for the last
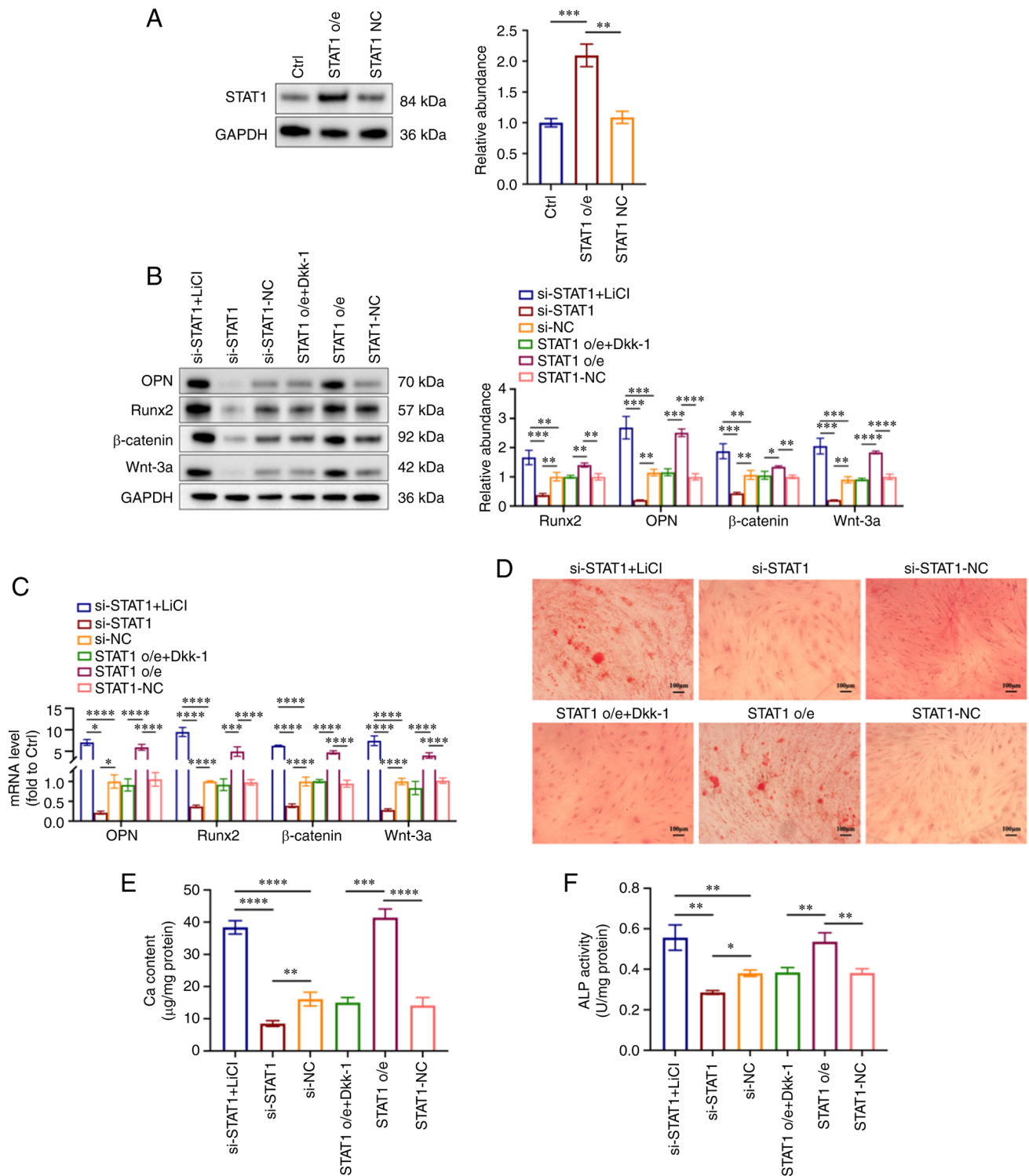
Figure 6. Wnt/β-catenin signaling pathway is involved in STAT1-mediated VSMC calcification. STAT1-overexpressing VSMCs were treated with 3 mM phosphorus for 7 days, with or without 100 ng/ml Dkk-1 added for the last 3 days of this period. si-STAT1 VSMCs were treated in the presence of 3 mM phosphorus for 7 days, with or without 5 mmol/l LiCl for the last 3 days of this period. (A) Expression levels of STAT1 in VSMCs were measured by western blot analysis. (B) Expression levels of OPN, Runx2, Wnt-3a and β-catenin were measured by western blot analysis. (C) Reverse transcription-quantitative PCR analysis of OPN, Runx2, Wnt-3a and β-catenin in VSMCs. (D) Mineralization was examined using Alizarin Red S staining. Scale bar, 100 μm. (E) Ca content in VSMCs was measured. (F) ALP activity was tested. *P<0.05, **P<0.01, ***P<0.001, ****P<0.0001. ALP, alkaline phosphatase; Ca, calcium; Ctrl, control; NC, negative control; o/e, overexpression; OPN, osteopontin; Runx2, runt-related transcription factor 2; si, small interfering RNA; VSMC, vascular smooth muscle cell; Dkk-1, Dickkopf-1; LiCl, lithium chloride.

3 days of this period. si-STAT1 VSMCs were treated in the presence of 3 mM phosphorus for 7 days, with or without 5 mmol/l LiCl (Wnt activator) added for the last 3 days of this period. The LiCl-treated si-STAT1 group (si-STAT1 + LiCl

group) exhibited increased expression levels of OPN, Runx2, Wnt-3a and β-catenin, while the Dkk-1-treated STAT1 o/e group (STAT1 o/e + DKK-1) displayed decreased expression at both the protein and gene levels (Fig. 6B and C). The Ca

deposition in cultured VSMCs was detected by Alizarin Red S staining. The LiCl-treated si-STAT1 group (si-STAT1 + LiCl group) exhibited more mineralized nodules compared with the si-STAT1 and si-NC groups, and the Dkk-1-treated STAT1 o/e group (STAT1 o/e + Dkk-1 group) exhibited fewer mineralized nodules compared with the STAT1 o/e group and STAT1-NC group (Fig. 6D). Similarly, the ALP and Ca contents were increased in the LiCl-treated si-STAT1 group (si-STAT1 + LiCl group) compared with si-STAT1 group and si-NC group, while they were decreased in the Dkk-1-treated STAT1 o/e group (STAT1 o/e + Dkk-1 group) compared with the STAT1 o/e group (Fig. 6E and F). These results suggested that LiCl reversed the protective effect of STAT1 inhibition on VSMC calcification and Dkk-1 alleviated the effect of STAT1 overexpression in HP-induced VSMC calcification.

Taken together, the present results indicated that exosomal STAT1 derived from HP-treated HUVECs promoted VSMC calcification by activating the Wnt/β-catenin signaling pathway.

Discussion

VC is associated with both cardiovascular and all-cause mortality in patients with CKD, and CKD-related VC commonly starts from the tunica media (1,10). However, the exact mechanism of how the calcification signal in circulating blood is transferred to the tunica media remains unknown. It is also unknown whether exosomes can mediate the interaction between ECs and VSMCs in a HP environment. In the present study, exosomes derived from HP-treated HUVECs could promote VSMC calcification. Higher expression of STAT1 was observed in HP-HUVEC-Exo compared with NP-HUVEC-Exo. Subsequently, si-STAT1, fludarabine or overexpression plasmid of STAT1 were used to knockdown, inhibit or upregulate STAT1 expression, respectively, and the promoting or inhibitory effects on calcification were observed. Finally, the present study further revealed that the Wnt-3a/β-catenin pathway may be the potential mechanism. In summary, the present study revealed that HP-stimulated HUVECs secreted exosomes, which carried the STAT1 protein to VSMCs, thus promoting the calcification of VSMCs via activation of the Wnt/β-catenin signaling pathway. The present findings demonstrated that exosomal STAT1 from ECs in HP environments may contribute to the calcification of VSMCs, indicating a potential role of exosomes in intercellular communication between ECs and VSMCs in CKD-related VC.

Exosomes are EVs derived from cells and serve as important intercellular message transporters (25,26). Previous studies have demonstrated that exosomes participate in the process of VC (27,28). Kapustin *et al* (13) reported the co-location of CD63 (a biomarker of exosomes) and the calcification site in the vessel wall, indicating the involvement of exosomes in VC. Exosomes can participate in VC formation by acting as mineralization sites for minerals such as Ca and phosphorus (29,30). Kapustin *et al* (31) observed that the mineralization of VSMC-derived matrix vesicles was a pathological response to disturbed intracellular Ca homeostasis that led to calcification inhibitor depletion and the formation of annexin A6/phosphatidylserine nucleation complexes. It also regulates the phenotypic conversion of VSMCs from a contractile to a synthetic state, thus contributing to vascular

pathologies, including VC, restenosis and atherosclerosis (7). Sortilin has been reported as a key transport factor that regulates VSMC calcification; it can be transformed into exosomes with calcification potential and participate in the formation of microcalcification (32). In addition, the cargos of exosomes, including RNA, cytokines, proteins and lipids, could be transported between cells via exosomes, thus serving an important role in intercellular communication during the process of VC (33). Xu *et al* (34) reported that exosomes from melatonin-treated VSMCs could alleviate the calcification and aging of VSMCs in a paracrine manner through an exosomal microRNA (miRNA/miR)-204/miR-211 cluster by targeting bone morphogenetic protein-2. Guo *et al* (35) investigated the mechanisms of bone marrow mesenchymal stem cell (BMSC)-derived exosomes in attenuating VC. They found that BMSC-derived exosomes alleviated HP-induced calcification in human aortic VSMCs by modifying miRNA profiles, and the mTOR, MAPK and Wnt signaling pathways were involved in this process (35). Similar to our study, Li *et al* (16) reported that exosomes from hyperglycemia-stimulated vascular ECs promoted the calcification and senescence of VSMCs through the transport of versican by inducing mitochondrial dysfunction. Exosomal Notch3 from high glucose-stimulated ECs has also been reported to promote VSMC calcification and aging, and the mTOR signaling pathway is closely related to the Notch3 protein and involved in regulating calcification and aging (20). The present results for PKH26-labeled exosomes demonstrated that exosomes from HUVECs were mainly located in the cytoplasm of VSMCs. Similarly, Li *et al* (36) also reported that exosomal circRTN4 from mesenchymal stem cells could alleviate sepsis-induced myocardial injury, and their fluorescence *in situ* hybridization assay results demonstrated the location of circRTN4 in the cytoplasm of cardiomyocytes. Although the details of exosome localization in the cytoplasm need to be further explored, the present study revealed that exosomes could serve as an important cargo transporter between HUVECs and VSMCs and are thus involved in the process of VC.

In addition, the present study demonstrated that STAT1 was enriched in exosomes derived from HP-stimulated HUVECs and served a key role in VC. STAT family members are potential cytoplasmic transcription factors that mediate a variety of biological responses, including cell proliferation, survival, apoptosis and differentiation (37). STAT1 can be activated by a variety of extracellular stimulators, such as Janus kinase, and then enters the nucleus and regulates the expression of target genes (38,39). STAT1 may also be involved in the development of VC (40-42). Smyth *et al* (40) reported that patients with a gain-of-function STAT1 mutation were more likely to have significant VC, in which progressive calcification of the aorta and aortic valve can even lead to constricted obstruction at the calcified site. Kuniga *et al* (41) revealed that the expression of STAT1 in VSMCs could be activated by adding monocyte-expressed urokinase, and the activation of STAT1 inhibited the proliferation of VSMCs. In another *in vitro* experiment, Demyanets *et al* (42) treated VSMCs with the STAT1 activator oncostatin-M (OSM). They found that OSM promoted the production and activation of STAT1 and then led to the loss of VSMC contractile phenotype, which is a typical feature of osteogenic VSMCs (42). Further

studies have demonstrated that the overexpression of STAT1 reduces VSMC contractile gene expression, thus leading to a reduced contractile phenotype and promoting VSMC dedifferentiation (43). Regarding cellular signaling communication between cells, Cossetti et al (44) revealed that interferon-γ (IFN-γ) could bind to EVs through the activation of STAT1 in target cells by IFN-γ receptor 1 (IFNGR1), indicating the role of STAT1 in intercellular communication. In addition, endogenous STAT1 and IFNGR1 in target cells were indispensable for the activation of STAT1 signaling via EV-related IFN-γ/IFNGR1 complexes, demonstrating the role of STAT1 in cellular signaling regulated by EVs (44). Cai et al (45) reported that exosomal miRNA-221 promoted the polarization of M1 macrophages through the upregulation of STAT1 and STAT3, thus suggesting a novel crosstalk signaling pathway between mammary epithelial cells and macrophages during inflammation. Similar to previous studies (40-43), it was also observed that high expression of STAT1 was involved in the calcification of VSMCs, suggesting that the inhibition of STAT1 may represent a novel therapeutic target for the control of vascular diseases such as calcification, atherosclerosis and restenosis.

The present results also demonstrated that vascular endothelial dysfunction may contribute to the calcification mechanism of vessels. The present study demonstrated that the initial endothelial dysfunction caused by HP could serve a key role in the progression of VC by releasing EVs. Under pathological stimuli, ECs secrete exosomes and transfer protein cargos, thus leading to the osteochondrogenic transdifferentiation of VSMCs followed by the formation of micro- and macrocalcification in the vessel wall (13,14,25). In vivo and in vitro studies have suggested that EVs serve a central role in promoting cellular dysfunction by directly interacting with the endothelium (46,47). EVs reduce nitric oxide (NO) bioavailability, inhibit endothelial NO synthase and activate ERK signaling under pathological conditions to impair vasorelaxation (48,49). There was a similar effect of circulating EVs on ECs in animal models that mimic diabetes-induced endothelial dysfunction, although the mechanisms were different (50). A higher level of arginase 1 (Arg1) was detected in circulating EVs from diabetic mice than in those from normoglycemic mice. It could reduce L-arginine availability, which is essential to NO production, by converting it to urea and ornithine (50). Therefore, circulating EVs transfer Arg1 to ECs, thus reducing NO and impairing vasorelaxation (50). In warfarin-treated rats, compromised basal NO availability/increased vessel tone was observed during the arterial media calcification process, and the L-N-nitro-arginine methyl ester-induced further deterioration of endothelial function was associated with the calcification process, indicating that the loss of endothelial function was associated with early stages of arterial media calcification development (51). In addition, the function of the endothelium is related to the activation of platelets and other biological processes (47). Grześk et al (52) compared the effects of low- and high-dose aspirin co-administered with ticagrelor on the reactivity of VSMCs and found that high-dose aspirin impaired the anticontractile effect of ticagrelor on ADP-induced VSMC contraction in a rat model. Additionally, a previous study also demonstrated the responses of VSMC contraction to phenylephrine, angiotensin II and mastoparan-7

modulated by endothelial function (53). Endothelium dysfunction serves a key role in the progression of VC; however, how it impacted VSMCs through exosomes in the present study still requires further research.

The Wnt/β-catenin pathway is widely reported to be associated with VC (54). Gaur et al (55) reported that Runx2 was a target gene of Wnt signaling, and the activation of Runx2 stimulated osteoblast differentiation and bone formation. Similarly, another study suggested that HP could activate Wnt/β-catenin signaling and activated Wnt/β-catenin signaling promoted VSMCs osteogenic transdifferentiation and calcification by directly modulating Runx2 gene expression (56). In our previous study, CKD rats showed more significant VC than rats in control group, and the expression levels of Wnt-3a and β-catenin at calcified sites were increased, which was positively associated with the tissue calcification score, suggesting that the activation of Wnt/β-catenin signaling was involved in VC in CKD (57). Wu et al (58) reported that miR-708-5p was inhibited and pituitary specific transcription factor-1 (Pit-1) was upregulated in HP-induced VC. Further experiments demonstrated that miR-708-5p could inactivate the Wnt8b/β-catenin pathway by targeting Pit-1 to alleviate HP-induced VC (58). Cong et al (59) found that related transcriptional enhancer factor could ameliorate β-glycerolphosphate-induced calcification and osteoblastic differentiation of VSMCs by inhibiting the Wnt/β-catenin signaling pathway. The interplay between STAT1 and the Wnt/β-catenin signaling pathway has also been reported before. Zhao et al (60) revealed that the downregulation of STAT1 could weaken the aggressiveness of glioblastoma cells through inhibition of epithelial-mesenchymal transition both in vivo and in vitro, which is mediated via the Wnt/β-catenin signaling pathway. Yuan et al (61) demonstrated that STAT1 could be recruited into the promoter of β-catenin to activate its expression, and this effect was regulated by IFN-γ. In epithelial ovarian cancer, STAT1 could promote the upregulation of long non-coding RNA LINC00958, thus accelerating tumorigenesis by modulating Wnt/β-catenin signaling (62). A similar cross-link of STAT1 and Wnt/β-catenin signaling was also observed in the present study. The overexpression of STAT1 promoted VSMC calcification, and the downregulation of STAT1 alleviated calcification. These effects were attenuated when Dkk-1 or LiCl was added to the VSMCs, suggesting the interplay of STAT1 and the Wnt/β-catenin signaling pathway in VC.

The present study first demonstrated that exosomes derived from HP-treated HUVECs could promote VSMC calcification. Then, the different protein cargos in exosomes were determined and the different expression of STAT1 between the HP-HUVEC-Exo and NP-HUVEC-Exo groups was further observed. Subsequently, si-STAT1, fludarabine or overexpression plasmid of STAT1 were used to knockdown, inhibit or upregulate STAT1 expression, respectively, and the promoting or inhibitory effects on calcification were observed. Finally, the present study further explored the potential signal pathway and found that the pro-calcified effect caused by HP-HUVEC-Exo may be associated with the Wnt-3a/β-catenin pathway. However, the inhibition of STAT1 in HUVECs or exosomes would further confirm the results, which should be performed in the future. Another limitation is that all experiments were conducted in vitro, and thus, further in vivo studies are still required.

In conclusion, exosomes enriched with STAT1 derived from HP-treated HUVECs could be transmitted to VSMCs, thus promoting the calcification of VSMCs by activating the Wnt/β-catenin signaling pathway, indicating that exosomal STAT1 might be a novel therapeutic direction in CKD-related VC. This finding highlights a novel method of intercellular communication between ECs and VSMCs and provides insights into the mechanism of VC in patients with CKD.

Acknowledgements

Funding

Availability of data and materials

The datasets generated and/or analyzed during the current study are available in the iProX repository, https://www.iprox.cn/page/project.html?id=IPX0005088000. All other datasets used and/or analyzed during the current study are available from the corresponding author on reasonable request.

Authors' contributions

ZQ, YL, JL and LJ performed the experiments and data analysis. ZZ, KC, QY and SC provided technical support and materials, and interpreted data. ZQ and RL contributed to manuscript writing. RL and BS contributed to the design of the experiments and revised the article. ZQ and RL confirm the authenticity of all the raw data. All authors read and approved the final manuscript.

Ethics approval and consent to participate

Not applicable.

Patient consent for publication

Not applicable.

Competing interests

The authors declare they have no competing interests.

References

1. Ren SC, Mao N, Yi S, Ma X, Zou JQ, Tang X and Fan JM: Vascular calcification in chronic kidney disease: An update and perspective. Aging Dis 13: 673-697, 2022.
2. Nelson AJ, Raggi P, Wolf M, Gold AM, Chertow GM and Roe MT: Targeting vascular calcification in chronic kidney disease. JACC Basic Transl Sci 5: 398-412, 2020.
3. Denker M, Boyle S, Anderson AH, Appel LJ, Chen J, Fink JC, Flack J, Go AS, Horwitz E, Hsu CY, *et al*: Chronic renal insufficiency cohort study (CRIC): Overview and summary of selected findings. Clin J Am Soc Nephrol 10: 2073-2083, 2015.
4. Dube P, DeRiso A, Patel M, Battepati D, Khatib-Shahidi B, Sharma H, Gupta R, Malhotra D, Dworkin L, Haller S and Kennedy D: Vascular calcification in chronic kidney disease: Diversity in the vessel wall. Biomedicines 9: 404, 2021.
5. Düsing P, Zietzer A, Goody PR, Hosen MR, Kurts C, Nickenig G and Jansen F: Vascular pathologies in chronic kidney disease: Pathophysiological mechanisms and novel therapeutic approaches. J Mol Med (Berl) 99: 335-348, 2021.
6. Wang XR, Zhang JJ, Xu XX and Wu YG: Prevalence of coronary artery calcification and its association with mortality, cardiovascular events in patients with chronic kidney disease: A systematic review and meta-analysis. Ren Fail 41: 244-256, 2019.
7. Lanzer P, Boehm M, Sorribas V, Thiriet M, Janzen J, Zeller T, St Hilaire C and Shanahan C: Medial vascular calcification revisited: Review and perspectives. Eur Heart J 35: 1515-1525, 2014.
8. Yamada S and Giachelli CM: Vascular calcification in CKD-MBD: Roles for phosphate, FGF23, and Klotho. Bone 100: 87-93, 2017.
9. Raggi P: Cardiovascular calcification in end stage renal disease. Contrib Nephrol 149: 272-278, 2005.
10. Chen J, Budoff MJ, Reilly MP, Yang W, Rosas SE, Rahman M, Zhang X, Roy JA, Lustigova E, Nessel L, *et al*: Coronary artery calcification and risk of cardiovascular disease and death among patients with chronic kidney disease. JAMA Cardiol 2: 635-643, 2017.
11. Fang Y, Ginsberg C, Sugatani T, Monier-Faugere MC, Malluche H and Hruska KA: Early chronic kidney disease-mineral bone disorder stimulates vascular calcification. Kidney Int 85: 142-150, 2014.
12. Toussaint ND, Pedagogos E, Tan SJ, Badve SV, Hawley CM, Perkovic V and Elder GJ: Phosphate in early chronic kidney disease: Associations with clinical outcomes and a target to reduce cardiovascular risk. Nephrology (Carlton) 17: 433-444, 2012.
13. Kapustin AN, Chatrou ML, Drozdov I, Zheng Y, Davidson SM, Soong D, Furmanik M, Sanchis P, De Rosales RT, Alvarez-Hernandez D, *et al*: Vascular smooth muscle cell calcification is mediated by regulated exosome secretion. Circ Res 116: 1312-1323, 2015.
14. Qin Z, Liao R, Xiong Y, Jiang L, Li J, Wang L, Han M, Sun S, Geng J, Yang Q, *et al*: A narrative review of exosomes in vascular calcification. Ann Transl Med 9: 579, 2021.
15. Pan W, Liang J, Tang H, Fang X, Wang F, Ding Y, Huang H and Zhang H: Differentially expressed microRNA profiles in exosomes from vascular smooth muscle cells associated with coronary artery calcification. Int J Biochem Cell Biol 118: 105645, 2020.
16. Li S, Zhan JK, Wang YJ, Lin X, Zhong JY, Wang Y, Tan P, He JY, Cui XJ, Chen YY, *et al*: Exosomes from hyperglycemia-stimulated vascular endothelial cells contain versican that regulate calcification/senescence in vascular smooth muscle cells. Cell Biosci 9: 1, 2019.
17. Huang A, Guo G, Yu Y and Yao L: The roles of collagen in chronic kidney disease and vascular calcification. J Mol Med (Berl) 99: 75-92, 2021.
18. Song X, Yang B, Qiu F, Jia M and Fu G: High glucose and free fatty acids induce endothelial progenitor cell senescence via PGC-1α/SIRT1 signaling pathway. Cell Biol Int 41: 1146-1159, 2017.
19. Liu H, Yuan L, Xu S and Wang K: Endothelial cell and macrophage regulation of vascular smooth muscle cell calcification modulated by cholestane-3beta, 5alpha, 6beta-triol. Cell Biol Int 31: 900-907, 2007.

20. Lin X, Li S, Wang YJ, Wang Y, Zhong JY, He JY, Cui XJ, Zhan JK and Liu YS: Exosomal Notch3 from high glucose-stimulated endothelial cells regulates vascular smooth muscle cells calcification/aging. Life Sci 232: 116582, 2019.

21. Luo Z, Sun Y, Qi B, Lin J, Chen Y, Xu Y and Chen J: Human bone marrow mesenchymal stem cell-derived extracellular vesicles inhibit shoulder stiffness via let-7a/Tgfbr1 axis. Bioact Mater 17: 344-359, 2022.

22. Zhang C, Wang XY, Zhang P, He TC, Han JH, Zhang R, Lin J, Fan J, Lu L, Zhu WW, et al: Cancer-derived exosomal HSPC111 promotes colorectal cancer liver metastasis by reprogramming lipid metabolism in cancer-associated fibroblasts. Cell Death Dis 13: 57, 2022.

23. Lee JH, Song J, Kim IG, You G, Kim H, Ahh JH and Mok H: Exosome-mediated delivery of transforming growth factor-β receptor 1 kinase inhibitors and toll-like receptor 7/8 agonists for combination therapy of tumors. Acta Biomater 141: 354-363, 2022.

24. Livak KJ and Schmittgen TD: Analysis of relative gene expression data using real-time quantitative PCR and the 2(-Delta Delta C(T)) method. Methods 25: 402-408, 2001.

25. Yang W, Zou B, Hou Y, Yan W, Chen T and Qu S: Extracellular vesicles in vascular calcification. Clin Chim Acta 499: 118-122, 2019.

26. Kalluri R and LeBleu VS: The biology, function, and biomedical applications of exosomes. Science 367: eaau6977, 2020.

27. Bano S, Tandon S and Tandon C: Emerging role of exosomes in arterial and renal calcification. Hum Exp Toxicol 40: 1385-1402, 2021.

28. Liberman M and Marti LC: Vascular calcification regulation by exosomes in the vascular wall. Adv Exp Med Biol 998: 151-160, 2017.

29. Bobryshev YV, Killingsworth MC, Huynh TG, Lord RS, Grabs AJ and Valenzuela SM: Are calcifying matrix vesicles in atherosclerotic lesions of cellular origin? Basic Res Cardiol 102: 133-143, 2007.

30. Bommanavar S, Hosmani J, Togoo RA, Baeshen HA, Raj AT, Patil S, Bhandi S and Birkhed D: Role of matrix vesicles and crystal ghosts in bio-mineralization. J Bone Miner Metab 38: 759-764, 2020.

31. Kapustin AN, Davies JD, Reynolds JL, McNair R, Jones GT, Sidibe A, Schurgers LJ, Skepper JN, Proudfoot D, Mayr M and Shanahan CM: Calcium regulates key components of vascular smooth muscle cell-derived matrix vesicles to enhance mineralization. Circ Res 109: e1-e12, 2011.

32. Goettsch C, Hutcheson JD, Aikawa M, Iwata H, Pham T, Nykjaer A, Kjolby M, Rogers M, Michel T, Shibasaki M, et al: Sortilin mediates vascular calcification via its recruitment into extracellular vesicles. J Clin Invest 126: 1323-1336, 2016.

33. Bardeesi ASA, Gao J, Zhang K, Yu S, Wei M, Liu P and Huang H: A novel role of cellular interactions in vascular calcification. J Transl Med 15: 95, 2017.

34. Xu F, Zhong JY, Lin X, Shan SK, Guo B, Zheng MH, Wang Y, Li F, Cui RR, Wu F, et al: Melatonin alleviates vascular calcification and ageing through exosomal miR-204/miR-211 cluster in a paracrine manner. J Pineal Res 68: e12631, 2020.

35. Guo Y, Bao S, Guo W, Diao Z, Wang L, Han X, Guo W and Liu W: Bone marrow mesenchymal stem cell-derived exosomes alleviate high phosphorus-induced vascular smooth muscle cells calcification by modifying microRNA profiles. Funct Integr Genomics 19: 633-643, 2019.

36. Li J, Jiang R, Hou Y and Lin A: Mesenchymal stem cells-derived exosomes prevent sepsis-induced myocardial injury by a CircRTN4/miR-497-5p/MG53 pathway. Biochem Biophys Res Commun 618: 133-140, 2022.

37. Kim HS and Lee MS: STAT1 as a key modulator of cell death. Cell Signal 19: 454-465, 2007.

38. Xin P, Xu X, Deng C, Liu S, Wang Y, Zhou X, Ma H, Wei D and Sun S: The role of JAK/STAT signaling pathway and its inhibitors in diseases. Int Immunopharmacol 80: 106210, 2020.

39. Dodington DW, Desai HR and Woo M: JAK/STAT-emerging players in metabolism. Trends Endocrinol Metab 29: 55-65, 2018.

40. Smyth AE, Kaleviste E, Snow A, Kisand K, McMahon CJ, Cant AJ and Leahy TR: Aortic calcification in a patient with a gain-of-function STAT1 mutation. J Clin Immunol 38: 468-470, 2018.

41. Kunigal S, Kusch A, Tkachuk N, Tkachuk S, Jerke U, Haller H and Dumler I: Monocyte-expressed urokinase inhibits vascular smooth muscle cell growth by activating Stat1. Blood 102: 4377-4383, 2003.

42. Demyanets S, Kaun C, Rychli K, Pfaffenberger S, Kastl SP, Hohensinner PJ, Rega G, Katsaros KM, Afonyushkin T, Bochkov VN, et al: Oncostatin M-enhanced vascular endothelial growth factor expression in human vascular smooth muscle cells involves PI3K-, p38 MAPK-, Erk1/2- and STAT1/STAT3-dependent pathways and is attenuated by interferon-γ. Basic Res Cardiol 106: 217-231, 2011.

43. Kirchmer MN, Franco A, Albasanz-Puig A, Murray J, Yagi M, Gao L, Dong ZM and Wijelath ES: Modulation of vascular smooth muscle cell phenotype by STAT-1 and STAT-3. Atherosclerosis 234: 169-175, 2014.

44. Cossetti C, Iraci N, Mercer TR, Leonardi T, Alpi E, Drago D, Alfaro-Cervello C, Saini HK, Davis MP, Schaeffer J, et al: Extracellular vesicles from neural stem cells transfer IFN-γ via Ifngr1 to activate Stat1 signaling in target cells. Mol Cell 56: 193-204, 2014.

45. Cai M, Shi Y, Zheng T, Hu S, Du K, Ren A, Jia X, Chen S, Wang J and Lai S: Mammary epithelial cell derived exosomal MiR-221 mediates M1 macrophage polarization via SOCS1/STATs to promote inflammatory response. Int Immunopharmacol 83: 106493, 2020.

46. Buffolo F, Monticone S, Camussi G and Aikawa E: Role of extracellular vesicles in the pathogenesis of vascular damage. Hypertension 79: 863-873, 2022.

47. Godo S and Shimokawa H: Endothelial functions. Arterioscler Thromb Vasc Biol 37: e108-e114, 2017.

48. Taguchi K, Hida M, Narimatsu H, Matsumoto T and Kobayashi T: Glucose and angiotensin II-derived endothelial extracellular vesicles regulate endothelial dysfunction via ERK1/2 activation. Pflugers Arch 469: 293-302, 2017.

49. Brodsky SV, Zhang F, Nasjletti A and Goligorsky MS: Endothelium-derived microparticles impair endothelial function in vitro. Am J Physiol Heart Circ Physiol 286: H1910-H1915, 2004.

50. Zhang H, Liu J, Qu D, Wang L, Wong CM, Lau CW, Huang Y, Wang YF, Huang H, Xia Y, et al: Serum exosomes mediate delivery of arginase 1 as a novel mechanism for endothelial dysfunction in diabetes. Proc Natl Acad Sci USA 115: E6927-E6936, 2018.

51. Van den Bergh G, Van den Branden A, Opdebeeck B, Fransen P, Neven E, De Meyer GRY, D'Haese PC and Verhulst A: Endothelial dysfunction aggravates arterial media calcification in warfarin administered rats. FASEB J 36: e22315, 2022.

52. Grześk G, Kozinski M, Tantry US, Wicinski M, Fabiszak T, Navarese EP, Grzesk E, Jeong YH, Gurbel PA and Kubica J: High-dose, but not low-dose, aspirin impairs anticontractile effect of ticagrelor following ADP stimulation in rat tail artery smooth muscle cells. Biomed Res Int 2013: 928271, 2013.

53. Bosman M, Krüger DN, Favere K, Wesley CD, Neutel CHG, Van Asbroeck B, Diebels OR, Faes B, Schenk TJ, Martinet W, et al: Doxorubicin impairs smooth muscle cell contraction: Novel insights in vascular toxicity. Int J Mol Sci 22: 12812, 2021.

54. Bundy K, Boone J and Simpson CL: Wnt signaling in vascular calcification. Front Cardiovasc Med 8: 708470, 2021.

55. Gaur T, Lengner CJ, Hovhannisyan H, Bhat RA, Bodine PV, Komm BS, Javed A, van Wijnen AJ, Stein JL, Stein GS and Lian JB: Canonical WNT signaling promotes osteogenesis by directly stimulating Runx2 gene expression. J Biol Chem 280: 33132-33140, 2005.

56. Cai T, Sun D, Duan Y, Wen P, Dai C, Yang J and He W: WNT/β-catenin signaling promotes VSMCs to osteogenic trans-differentiation and calcification through directly modulating Runx2 gene expression. Exp Cell Res 345: 206-217, 2016.

57. Liao R, Wang L, Li J, Sun S, Xiong Y, Li Y, Han M, Jiang H, Anil M and Su B: Vascular calcification is associated with Wnt-signaling pathway and blood pressure variability in chronic kidney disease rats. Nephrology (Carlton) 25: 264-272, 2020.

58. Wu N, Liu GB, Zhang YM, Wang Y, Zeng HT and Xiang H: MiR-708-5p/Pit-1 axis mediates high phosphate-induced calcification in vascular smooth muscle cells via Wnt8b/β-catenin pathway. Kaohsiung J Med Sci 38: 653-661, 2022.

59. Cong J, Cheng B, Liu J and He P: RTEF-1 inhibits vascular smooth muscle cell calcification through regulating Wnt/β-catenin signaling pathway. Calcif Tissue Int 109: 203-214, 2021.

60. Zhao L, Li X, Su J, Wang Gong F, Lu J and Wei Y: STAT1 determines aggressiveness of glioblastoma both in vivo and in vitro through wnt/β-catenin signalling pathway. Cell Biochem Funct 38: 630-641, 2020.

61. Yuan X, He F, Zheng F, Xu Y and Zou J: Interferon-gamma facilitates neurogenesis by activating Wnt/β-catenin cell signaling pathway via promotion of STAT1 regulation of the β-catenin promoter. Neuroscience 448: 219-233, 2020.

62. Xie M, Fu Q, Wang PP and Cui YL: STAT1-induced upregulation lncRNA LINC00958 accelerates the epithelial ovarian cancer tumorigenesis by regulating Wnt/β-catenin signaling. Dis Markers 2021: 1405045, 2021.